Learning Dual Transformation Networks for Image Contrast Enhancement

Yurui Zhu, Xueyang Fu, and Aiping Liu

***Abstract*—In this work, we introduce a dual transformation network for single image contrast enhancement, which usually aims to improve global contrast and enrich local details. To this end, we propose two parallel branches to respectively handle the two goals by learning different kinds of transformations. Specifically, one branch aims to construct a global transformation curve to improve global contrast, while the other one directly predicts pixel offsets to enrich local details. In addition, we further design a differentiable histogram loss to provide supervised information related to the global contrast. In this way, the network training can be guided by different constraints, e.g., pixel-level mean squared error and statistics-level histogram error. Experiments demonstrate that our method can be effectively applied to various contrast conditions with favorable performance against the state-of-the-art methods.**

***Index Terms*—Image processing, contrast enhancement, deep learning, histogram equalization, CNNs.**

I. Introduction

IMAGE enhancement is an important task in the image processing field, which including many aspects, e.g., photo restoration [1] and low-light enhancement [2], [3]. For the low-contrast image, even at different brightness, the histogram is mostly distributed in a smaller dynamic range. This makes the captured image contain various degradations, e.g., low visibility, low contrast and hidden details. Therefore, improving image contrast can not only promote visual quality but also serve as a pre-processing for downstream computer vision tasks, e.g., object detection and medical image diagnosis.

Previous contrast enhancement methods can be roughly divided into two categories: 1-D histogram-based methods and 2-D histogram-based methods. The first category of enhancement methods [4]–[11] focus on 1-D histogram analysis. For instance, the classical histogram equalization (HE) [4] adopts the cumulative distribution function of the image histogram as its mapping function. This makes HE simple and easy to implement, but usually leads to over-enhancement. Exact histogram specification (EHS) [6] attempts to transform the input histogram to the sample distribution. The histogram modification framework [7] aims to output modified histogram by optimizing a specifically designed objective function. By adjusting the coefficients in the objective function, different levels of enhancement would be achieved. Automatic robust image contrast enhancement (RICE) [8] combines the original input, HE enhanced image, and a sigmoid transferred version to obtain the properly higher quality image. Brightness preserving dynamic histogram equalization (BPDHE) [9] aims to divide the input image histogram into several partitions applied with HE independently. Brightness preserving dynamic fuzzy histogram equalization (BPDFHE) [10], which is based on BPDHE, utilizes fuzzy statistics of digital images to represent images. Adaptive gamma correction with weighting distribution (AGCWD) [11] progressively increases the low intensity to avoid adverse effect. Recursive mean separate histogram equalization (RMSHE) [5] utilizes recursive operation to produce sub-histograms, then equalizes each sub-histogram.

2-D histogram-based methods usually utilize the inter-pixel contextual information to obtain enhanced images. Contextual and variational contrast enhancement algorithm (CVC) [12] constructs a 2-D histogram of an input image to create mapping function to generate the desired output. Two-dimensional histogram equalization (2DHE) [13] needs to fine-tune the size of the spatial neighborhood to achieve visually pleasing output. Layered difference representation (LDR) [14] represents the gray-level differences in a pyramid structure and magnifies the gray-level difference. In method [15], the optimization goal is to preserve the shape of the 1-D histogram and amplify the gray-level differences among adjacent pixels. In method [16], the authors design the spatial entropy and global mapping curve to achieve contrast enhancement. In method [17], the authors combine PageRank algorithm and spatial mutual information to handle contrast enhancement.

Early approaches either design global transformation functions or attempt to maximize the difference between adjacent pixels in the local regions. These hand-crafted methods usually have various problems while enhancing the image contrast. For instance, HE tends to amplify the latent noise in the image and bring unwanted artifacts, while AGCWD could not obtain the desired visual effect. Recently, with the development of data-driven deep learning, many low-level vision tasks achieved great success in the field of single image restoration, e.g., image de-noising [18], super-resolution [19], etc. However, during our experiments, we found that directly using deep convolutional neural networks, e.g., methods [18][19], cannot obtain satisfactory results. This illustrates that using plain CNNs that focus

Manuscript received September 16, 2020; revised October 26, 2020; accepted November 2, 2020. Date of publication November 5, 2020; date of current version November 24, 2020. This work was supported by the National Natural Science Foundation of China under Grant 61701158 and Grant 61901433. The associate editor coordinating the review of this manuscript and approving it for publication was Prof. Dezhong Peng. *(Corresponding author: Xueyang Fu.)*

The authors are with the University of Science and Technology of China, Hefei 230026, China (e-mail: zyr@mail.ustc.edu.cn; xyfu@ustc.edu.cn; aipingl@ustc.edu.cn).

Digital Object Identifier 10.1109/LSP.2020.3036312

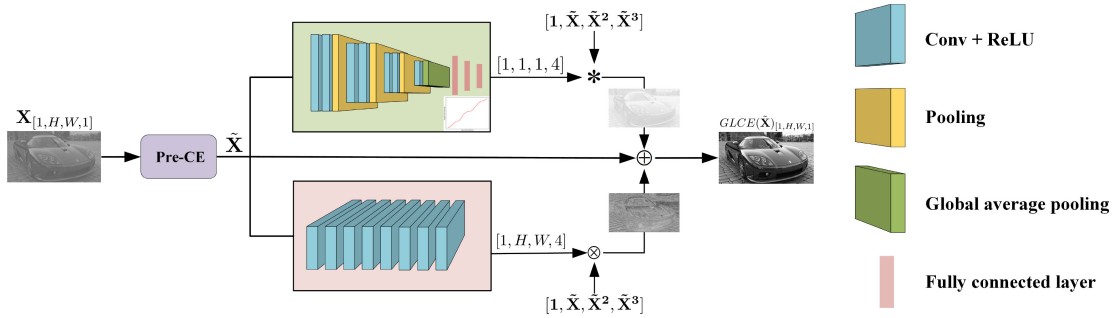

Fig. 1. The overall architecture of our proposed contrast enhancement network. All notations are the same as the paper. We also visualize the intermediate results. ($*$: Matrix multiplication; $\otimes$: Pixel-wise multiplication; $\oplus$: Pixel-wise addition).

only on local spatial information is not suitable for solving the specific contrast enhancement task.

In addition, we notice that the low-light image enhancement [20]–[25] is similar to the contrast enhancement task. In general, images captured in insufficient lighting environment suffer from loss of detail and reduced contrast. Most low-light image enhancement algorithms aim to adjust low-intensity pixels to improve contrast and restore sharp results. However, there are also low contrast in images taken under normal exposure and overexposure conditions. Since existing low-light enhancement methods mainly focus on processing low-intensity pixels, directly using these methods cannot well handle various low contrast images. To verify this viewpoint, we have retrained several deep learning-based models [20], [26]–[28] and test a model-based method [29] on the low-contrast database [30]. Experimental section shows that all these methods cannot be effectively generalized to different types of low-contrast images.

To address the above problems, we design a novel network to simultaneously improve global contrast and local details in a parallel fashion. Our contributions are summarized as follows:

1) We propose a new deep network architecture for single image contrast enhancement. Different from existing deep CNNs-based methods, which mainly adopt standard convolutional operations and explore local features for image restoration, we take both global and local transformations into consideration. This makes our model more suitable for the specific contrast enhancement task.
2) We design a differentiable loss function based on the image histogram distribution. In this way, the convergence direction of network training can be jointly determined from the the global histogram error and local pixel error.
3) Our method generalizes well to various contrast conditions and has a fast inference time. Experiments demonstrate that our model outperforms state-of-the-art methods qualitatively and quantitatively.

II. Methodology

We present our network in Figure 1. Our Global and Local Contrast Enhancement (GLCE) network consists of one Pre-CE module, one Global-CE module, and one Local-CE module. The framework applies both global and local mapping functions to the input low-contrast image. The final enhanced result is obtained by adding these two mapped results to the input image. Below we detail our GLCE network.

A. Pre-CE Module

We first utilize range standardization as the pre-processing:

$$\tilde{\mathbf{X}} = \frac{\mathbf{X} - \min(\mathbf{X})}{\max(\mathbf{X}) - \min(\mathbf{X})}, \tag{1}$$

where $\mathbf{X}$ is the low-contrast input and $\tilde{\mathbf{X}}$ is the pre-enhanced result. $\max(\cdot)$ and $\min(\cdot)$ are two operations to extract maximum and minimum values of $\mathbf{X}$, respectively.

B. Global and Local Enhancement Networks

Our proposed contrast enhancement model contains two sub-networks. We use $G(\cdot)$ and $L(\cdot)$ to denote global and local enhancement network, respectively. To increase network nonlinearity, we set $V(\tilde{\mathbf{X}})$ as a basis vector and is defined as $[\mathbf{1}, \tilde{\mathbf{X}}, \tilde{\mathbf{X}}^2, \tilde{\mathbf{X}}^3]$. Here $\tilde{\mathbf{X}}^2 = \tilde{\mathbf{X}} \otimes \tilde{\mathbf{X}}$ and $\tilde{\mathbf{X}}^3 = \tilde{\mathbf{X}} \otimes \tilde{\mathbf{X}} \otimes \tilde{\mathbf{X}}$, where $\otimes$ is pixel-wise multiplication. We generate an all-ones matrix $\mathbf{1}$ with same size as $\tilde{\mathbf{X}}$. Finally, $V(\tilde{\mathbf{X}})$ is the concatenation of the four matrices along the channel dimension.

For the global parameter network, the sub-network $G(\cdot)$ predicts a coefficient matrix $\theta_{\mathbf{G}} \in \mathbb{R}^{1\times 4}$ to enhance global contrast. Specifically, the output of global network is:

$$\tilde{\mathbf{X}}_G = G(\tilde{\mathbf{X}}) * V(\tilde{\mathbf{X}}) = \theta_{\mathbf{G}} * V(\tilde{\mathbf{X}}), \tag{2}$$

where $*$ denotes matrix multiplication. Similarity, the local parameter network $L(\cdot)$ also outputs a coefficient matrix θ_L, which has the same shape with $V(\tilde{\mathbf{X}})$, and is applied to multiply $V(\tilde{\mathbf{X}})$ at the pixel-level to enrich local details:

$$\tilde{\mathbf{X}}_L = \sum L(\tilde{\mathbf{X}}) \otimes V(\tilde{\mathbf{X}}) = \sum \theta_{\mathbf{L}} \otimes V(\tilde{\mathbf{X}}), \tag{3}$$

In addition, we utilize the residual learning strategy, which is supposed to speed up training, to obtain the final result:

$$GLCE(\tilde{\mathbf{X}}) = \tilde{\mathbf{X}} + \tilde{\mathbf{X}}_L + \tilde{\mathbf{X}}_G. \tag{4}$$

C. Training Loss

In many CNN methods for image processing, the most widely used loss function is MSE. Assuming N training image pairs $\{\mathbf{X}_i, \mathbf{T}_i\}_{i=1}^N$, where $\mathbf{X}_i$ represents the i-th low contrast image in

the training database, and $\mathbf{T}_i$ denotes the corresponding ground truth image. The training aims to minimize:

$$\mathcal{L}_{MSE} = \frac{1}{N}\sum_{i=1}^{N} \|\Phi(\mathbf{X}_i) - \mathbf{T}_i\|_2^2, \tag{5}$$

where $\Phi(\cdot)$ denotes GLCE network. Meanwhile, we adopt a local loss [31] to perform local constraints by randomly sampling several small areas from the outputs and labels:

$$\mathcal{L}_{local} = \frac{1}{MN}\sum_{i=1}^{N}\sum_{j=1}^{M} \|\phi(\Phi(\mathbf{X}_i)) - \phi(\mathbf{T}_i)\|_2^2, \tag{6}$$

where $\phi(\cdot)$ denotes the operation of randomly sampling M image patches with size of 256×256.

Furthermore, we specifically design a differentiable histogram loss to guide the global contrast enhancement:

$$\mathcal{L}_{hist} = \frac{1}{N}\sum_{i=1}^{N} \|Hist(\Phi(\mathbf{X}_i)) - Hist(\mathbf{T}_i)\|_1, \tag{7}$$

where $Hist(\cdot)$ denotes the extracted histogram distribution. The image histogram counts the number of pixels in each discrete range of intensity values, which belongs to the image global statistical information. However, the calculation process of the original image histogram is not differentiable, which cannot be used for network training. Therefore, we imitate histogram distribution by using kernel density estimation [32] to construct a differentiable histogram, which can participate in the back propagation process to update the parameters.

In the parallel network structure, since $L(\tilde{\mathbf{X}})$ provides pixel offset values, this may introduce significant discontinuities at the edges of the image. Therefore, the gradient loss $\mathcal{L}_{grad}$ is introduced to avoid artifacts and preserve image structural information in the enhanced image. $\mathcal{L}_{grad}$ is defined as:

$$\mathcal{L}_{grad} = \frac{1}{N}\sum_{i=1}^{N} \|\nabla(\Phi(\mathbf{X}_i)) - \nabla(\mathbf{T}_i)\|_2, \tag{8}$$

where ∇ denotes the difference in the horizontal and vertical directions. Finally, the total loss is:

$$\mathcal{L}_{total} = \alpha_1\mathcal{L}_{MSE} + \alpha_2\mathcal{L}_{local} + \alpha_3\mathcal{L}_{hist} + \alpha_4\mathcal{L}_{grad}, \tag{9}$$

where α_1 , α_2 , α_3 and α_4 are the weights of the losses.

III. Experiment Results

A. Implementation Details

We implement our GLCE[1] in Tensorflow on a PC with an Nvidia GTX 1080Ti GPU. Our model is trained for 240 epochs by using the Adam optimizer [33] with a learning rate of 10^{-4}. All convolutional kernels size is 3×3. We take two different inputs for each sub-network. For the local network, we directly input the normalized images $\tilde{\mathbf{X}}$, while a 256×256 scaled version of $\tilde{\mathbf{X}}$ is used for the global network. Hence the network can perform the mapping transformation for arbitrary resolution. We set the batch size to 1, and the setting of loss function weights are empirically set as: $\alpha_1 = 1$, $\alpha_2 = 5$, $\alpha_3 = 2 \times 10^3$, and $\alpha_4 = 0.5$. For the training data, we use 1477 pairs of low contrast gray-scale images and their ground truth versions, including $CCID$ [34] database and our synthesized images. For color image, the process can be firstly performed in the Y channel of YUV color space, and then convert the result back to RGB space.

[1]Our source code is available at https://github.com/zhuyr97/GLCE.

TABLE I
Quantitative Comparisons on MAD Database. MAD_{gray} Denotes the Gray-Scale Versions. Red and Blue Indicate the Best and Second Best Results, Respectively

Methods	MAD_{gray}				MAD			
	PSNR	SSIM	PCQI	NIQE	PSNR	SSIM	PCQI	NIQE
HE [4]	16.99	0.731	1.157	4.186	17.48	0.736	1.184	4.001
Tarik [7]	23.26	0.860	1.129	3.982	22.51	0.844	1.111	3.767
RICE [8]	23.53	0.813	1.157	3.969	22.55	0.802	1.133	4.011
BPDHE [9]	23.07	0.817	1.158	4.118	21.32	0.795	1.134	3.934
BPDFHE [10]	21.58	0.777	1.051	4.088	20.58	0.749	1.059	4.107
AGCWD [11]	16.56	0.722	1.033	4.229	17.21	0.720	1.025	4.107
RMSHE [5]	21.35	0.778	1.191	3.627	13.68	0.394	1.190	3.651
CVC [12]	19.29	0.808	1.184	3.845	19.12	0.807	1.139	3.726
2DHE [13]	19.45	0.835	1.205	3.842	18.91	0.820	1.171	3.915
LDR [14]	26.83	0.948	1.056	3.746	24.27	0.931	1.038	3.667
COTH [15]	19.32	0.827	0.988	3.903	18.80	0.812	1.038	3.691
SECE [16]	29.21	0.951	1.199	3.737	24.99	0.920	0.181	3.630
Celik [17]	22.68	0.907	1.191	3.713	21.49	0.886	1.161	3.713
DnCNN [18]	22.77	0.794	1.026	4.041	21.83	0.786	1.024	4.017
RDN [19]	19.51	0.748	0.971	3.967	19.01	0.735	0.979	4.028
RetinexNet [26]	10.83	0.634	0.817	4.709	11.42	0.642	0.849	4.500
GLAD-Net [27]	13.23	0.649	0.776	4.189	13.42	0.630	0.806	4.226
KinD [20]	18.37	0.818	1.201	3.735	19.72	0.841	1.191	3.539
Zhang et al. [29]	13.78	0.711	0.936	3.915	12.78	0.701	0.982	3.890
Ours	31.71	0.949	1.208	3.558	25.89	0.927	1.199	3.546

B. Results on Testing Database

We utilize the MAD [30] database as our testing data. MAD is a dedicated contrast changed color image database with distorted images and their corresponding ground truth versions. Note that this database does not participate in the training process. We adopt four objective IQA as our evaluation metrics, including three full-reference methods, peak signal-to-noise ratio (PSNR), structural similarity (SSIM) [35] and patch-based contrast image quality index (PCQI) [36]. Higher PSNR and SSIM values generally indicate the enhanced image is closer to the ground truth. PCQI, which is a reduced-reference quality assessment, specially evaluates perceptual images quality based on an adaptive representation of local patch structure between the input and output. The Natural Image Quality Evaluator (NIQE) [37], is a no-reference quality assessment based on natural scene statistical features. Larger PCQI and smaller NIQE values indicate a higher quality.

As shown in Table I, our method shows superiority than other comparison methods on overall performance. We also show one visual comparison in Figure 2, and it is clear that other comparison methods cannot well process the input image. For example, the deep low-light model KinD [20] obviously improves the image brightness. However, the distribution range of pixel values is concentrated, which leads to a relatively low contrast. Other contrast enhancement methods, such as SECE [16], have slight over-enhancement in the enhanced result. This is because these methods tend to make gray levels to cover the entire dynamic range. On the contrary, our method achieves promising results in both objective and subjective evaluations.

Since our network requires only one forward pass after training, it has a fast inference time. Table II shows the comparisons

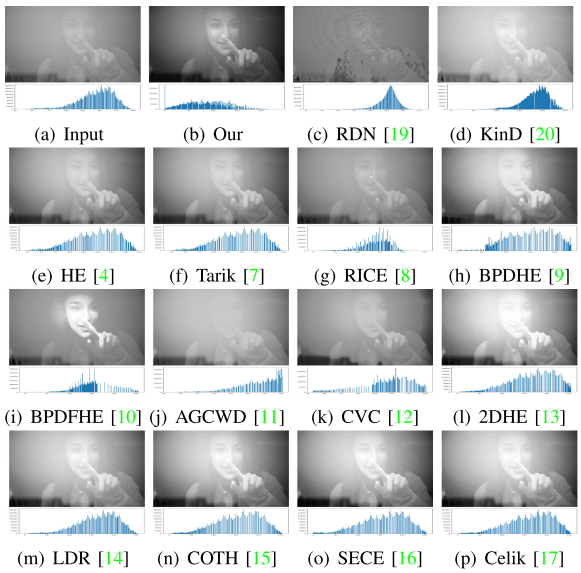

Fig. 2. Visual comparison with state-of-the-art methods.

TABLE II
COMPARISON ON INFERENCE TIME (SECONDS)

Image size	Average inference time					
	Tarik [7]	RICE [8]	LDR [14]	SECE [16]	Celik [17]	ours
512×512	0.26	0.32	0.39	0.76	1.08	0.15
1700×1700	1.13	0.84	2.45	6.20	9.53	0.49

TABLE III
AVERAGE SCORES OF USER STUDY

	HE [4]	LDR [14]	SECE [16]	2DHE [13]	Our
Scores	1.61	3.11	3.74	2.47	4.16

on average inference time for two different image sizes, each averaged over 10 testing images.

C. User Study

We also construct a user study to provide realistic feedback by randomly selecting 12 images from testing database. First, each image is enhanced by five methods i.e., HE, 2DHE, LDR, SECE and our model. Then, we ask 6 subjects to independently evaluate the results in a pairwise manner from two aspects: (1) whether the images show artifacts or nonrealistic distortions; (2) whether the images contain over- or under-enhancement in terms of contrast. Every method's results are assigned with score 1-5, where 5 means best. Finally, we average the scores showed in Table III, and the results give additional support along with NIQE that our network improves visual qualities on enhanced images.

D. Ablation Study

We conduct ablation studies to better analyze our network.

1) Effects of $\mathcal{L}_{hist}$ and $\mathcal{L}_{grad}$: Since $\mathcal{L}_{MSE}$ and $\mathcal{L}_{local}$ have been widely used and discussed in low-level vision tasks [18], [31], here we only focus on $\mathcal{L}_{hist}$ and $\mathcal{L}_{grad}$. As shown in Figure 3(b), without using $\mathcal{L}_{grad}$, obvious artifacts can be observed on the edges, and many glitches are reflected on the corresponding histogram distribution. While in Figure 3(c), without using $\mathcal{L}_{hist}$, the dynamic range of gray levels is not well expanded, resulting in insignificant enhancement effects. The best visual quality is obtained by using all the loss functions, as shown in Figure 3(d).

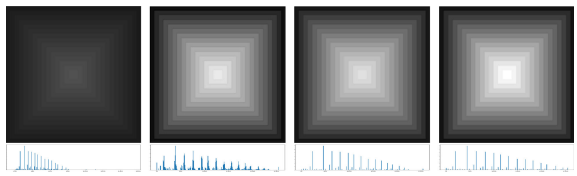

Fig. 3. Ablation study on loss functions.

TABLE IV
EFFECTS OF THE PRE-CE MODULE

	MAD_{gray}				MAD			
	PSNR	SSIM	PCQI	NIQE	PSNR	SSIM	PCQI	NIQE
w/o Pre-CE	25.47	0.892	1.139	3.609	23.22	0.873	1.112	3.629
w/ Pre-CE	31.71	0.949	1.208	3.558	25.89	0.927	1.199	3.546

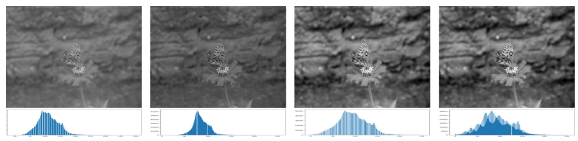

Fig. 4. Ablation study on modules.

2) Effects of the Three Modules: We re-train our models to verify the effects of the three modules. We first test the effect of the Pre-CE module and show the results in Table IV. Before the network training, utilizing the Pre-CE module has the following advantages: First, it can speed up the convergence of the sub-networks since the dynamic range is stretched, which reduces the degree of variation of the histogram. Second, range standardization can well maintain the shape of the histogram, which does not change the relative order of pixel values. Therefore, utilizing range standardization can provide a better initial input for the network.

After preprocessing, one visual comparison result about the global and local modules is shown in Figure 4. As can be seen in Figure 4(b), using only the local module have a slight improvement in global contrast. While using only the global module results in a noticeable global contrast enhancement, as shown in Figure 4(c). By jointly using the three modules, both enhanced contrast and sharpness can be simultaneously achieved, as shown in Figure 4(d).

IV. CONCLUSION

In this work, we propose a new deep network architecture, which contains two parallel branches for single image contrast enhancement. The global branch learns a cubic mapping curve for the entire image transformation to improve global contrast. The local branch attempts to enhance detail information by providing a pixel-level transformation. Compared with existing methods, our method not only maintains the 1-D input histogram shape, but also obtains better 2-D image visual quality. Our future work will extend our model to the color restoration, noise reduction and compression artifacts suppression.

REFERENCES

[1] H. Zeng, J. Cai, L. Li, Z. Cao, and L. Zhang, "Learning image-adaptive 3D lookup tables for high performance photo enhancement in real-time," *IEEE Trans. Pattern Anal. Mach. Intell.*, early access, Sep. 25, 2020, doi: 10.1109/TPAMI.2020.3026740.

[2] X. Ren, W. Yang, W. Cheng, and J. Liu, "Lr3m: Robust low-light enhancement via low-rank regularized retinex model," *IEEE Trans. Image Process.*, vol. 29, pp. 5862–5876, 2020.

[3] M. Fan, W. Wang, W. Yang, and J. Liu, "Integrating semantic segmentation and retinex model for low-light image enhancement," in *Proc. ACM Int. Conf. Multimedia*, Oct. 2020, pp. 2317–2325.

[4] R. C. Gonzalez and R. E. Woods, *Digital Image Processing*, 3rd ed., London, U.K.: Pearson, 2014.

[5] S.-D. Chen and A. Ramli, "Contrast enhancement using recursive mean-separate histogram equalization for scalable brightness preservation," *IEEE Trans. Consum. Electron.*, vol. 49, no. 4, pp. 1301–1309, Nov. 2003.

[6] D. Coltuc, P. Bolon, and J.-M. Chassery, "Exact histogram specification," *IEEE Trans. Image Process.*, vol. 15, no. 5, pp. 1143–1152, May 2006.

[7] T. Arici, S. Dikbas, and Y. Altunbasak, "A histogram modification framework and its application for image contrast enhancement," *IEEE Trans. Image Process.*, vol. 18, no. 9, pp. 1921–1935, Sep. 2009.

[8] K. Gu, G. Zhai, X. Yang, W. Zhang, and C. W. Chen, "Automatic contrast enhancement technology with saliency preservation," *IEEE Trans. Circuits Syst. Video Technol.*, vol. 25, no. 9, pp. 1480–1494, Sep. 2015.

[9] H. Ibrahim and N. Kong, "Brightness preserving dynamic histogram equalization for image contrast enhancement," *IEEE Trans. Consum. Electron.*, vol. 53, no. 4, pp. 1752–1758, Nov. 2007.

[10] D. Sheet, H. Garud, A. Suveer, M. Mahadevappa, and J. Chatterjee, "Brightness preserving dynamic fuzzy histogram equalization," *IEEE Trans. Consum. Electron.*, vol. 56, no. 4, pp. 2475–2480, Nov. 2010.

[11] S.-C. Huang, F.-C. Cheng, and Y.-S. Chiu, "Efficient contrast enhancement using adaptive gamma correction with weighting distribution," *IEEE Trans. Image Process.*, vol. 22, no. 3, pp. 1032–1041, Mar. 2013.

[12] T. Celik and T. Tjahjadi, "Contextual and variational contrast enhancement," *IEEE Trans. Image Process.*, vol. 20, no. 12, pp. 3431–3441, Dec. 2011.

[13] T. Celik, "Two-dimensional histogram equalization and contrast enhancement," *Pattern Recognit.*, vol. 45, no. 10, pp. 3810–3824, Oct. 2012.

[14] C. Lee, C. Lee, and C.-S. Kim, "Contrast enhancement based on layered difference representation of 2D histograms," *IEEE Trans. Image Process.*, vol. 22, no. 12, pp. 5372–5384, Dec. 2013.

[15] D. Kim and C. Kim, "Contrast enhancement using combined 1-D and 2-D histogram-based techniques," *IEEE Signal Process. Lett.*, vol. 24, no. 6, pp. 804–808, Jun. 2017.

[16] T. Celik, "Spatial entropy-based global and local image contrast enhancement," *IEEE Trans. Image Process.*, vol. 23, no. 12, pp. 5298–5308, Dec. 2014.

[17] T. Celik, "Spatial mutual information and pagerank-based contrast enhancement and quality-aware relative contrast measure," *IEEE Trans. Image Process.*, vol. 25, no. 10, pp. 4719–4728, Oct. 2016.

[18] K. Zhang, W. Zuo, Y. Chen, D. Meng, and L. Zhang, "Beyond a Gaussian denoiser: Residual learning of deep CNN for image denoising," *IEEE Trans. Image Process.*, vol. 26, no. 7, pp. 3142–3155, Jul. 2017.

[19] Y. Zhang, Y. Tian, Y. Kong, B. Zhong, and Y. Fu, "Residual dense network for image super-resolution," in *Proc. IEEE/CVF Conf. Comput. Vis. Pattern Recognit.*, 2018, pp. 2472–2481.

[20] Y. Zhang, J. Zhang, and X. Guo, "Kindling the darkness: A practical low-light image enhancer," in *Proc. ACM Int. Conf. Multimedia*, Oct. 2019, pp. 1632–1640.

[21] K. G. Lore, A. Akintayo, and S. Sarkar, "LLNet: A deep autoencoder approach to natural low-light image enhancement," *Pattern Recognit.*, vol. 61, pp. 650–662, Jan. 2017.

[22] R. Wang, Q. Zhang, C.-W. Fu, X. Shen, W.-S. Zheng, and J. Jia, "Underexposed photo enhancement using deep illumination estimation," in *Proc. IEEE/CVF Conf. Comput. Vis. Pattern Recognit.*, 2019, pp. 6842–6850.

[23] C. Li, J. Guo, F. Porikli, and Y. Pang, "LightenNet: A convolutional neural network for weakly illuminated image enhancement," *Pattern Recognit. Lett.*, vol. 104, pp. 15–22, 2018.

[24] W. Yang, Y. Yuan, W. Ren, J. Liu, W. J. Scheirer *et al.*, "Advancing image understanding in poor visibility environments: A collective benchmark study," *IEEE Trans. Image Process.*, vol. 29, pp. 5737–5752, 2020.

[25] L. Wang, Z. Liu, W. Siu, and D. P. K. Lun, "Lightening network for low-light image enhancement," *IEEE Trans. Image Process.*, vol. 29, pp. 7984–7996, 2020.

[26] W. Y. J. L. Chen Wei and Wenjing Wang, "Deep retinex decomposition for low-light enhancement," in *Proc. Brit. Mach. Vis. Conf.*, 2018, pp. 1–12.

[27] W. Wang, C. Wei, W. Yang, and J. Liu, "GladNet: Low-light enhancement network with global awareness," in *Proc. 13th IEEE Int. Conf. Autom. Face Gesture Recognit.*, 2018, pp. 751–755.

[28] H. Lee, K. Sohn, and D. Min, "Unsupervised low-light image enhancement using bright channel prior," *IEEE Signal Process. Lett.*, vol. 27, pp. 251–255, 2020.

[29] Q. Zhang, G. Yuan, C. Xiao, L. Zhu, and W.-S. Zheng, "High-quality exposure correction of underexposed photos," in *Proc. ACM Int. Conf. Multimedia*, Oct. 2018, pp. 582–590.

[30] E. C. Larson and D. M. Chandler, "Most apparent distortion: Full-reference image quality assessment and the role of strategy," *J. Electron. Imag.*, vol. 19, no. 1, 2010, Art. no. 11006.

[31] Y. Jiang *et al.*, "EnlightenGAN: Deep light enhancement without paired supervision," pp. 1–11, Jun. 2019, *arXiv:1906.06972*.

[32] Z. I. Botev *et al.*, "Kernel density estimation via diffusion," *Ann. Statist.*, vol. 38, no. 5, pp. 2916–2957, 2010.

[33] D. P. Kingma and J. L. Ba, "Adam: A method for stochastic optimization," in *Proc. Int. Conf. Learn. Representations*, 2015, pp. 1–15.

[34] K. Gu, G. Zhai, W. Lin, and M. Liu, "The analysis of image contrast: From quality assessment to automatic enhancement," *IEEE Trans., Cybern.*, vol. 46, no. 1, pp. 284–297, Jan. 2016.

[35] Z. Wang, A. C. Bovik, H. R. Sheikh, and E. P. Simoncelli, "Image quality assessment: From error visibility to structural similarity," *IEEE Trans. Image Process.*, vol. 13, no. 4, pp. 600–612, Apr. 2004.

[36] S. Wang, K. Ma, H. Yeganeh, Z. Wang, and W. Lin, "A patch-structure representation method for quality assessment of contrast changed images," *IEEE Signal Process. Lett.*, vol. 22, no. 12, pp. 2387–2390, Dec. 2015.

[37] A. Mittal, R. Soundararajan, and A. C. Bovik, "Making a completely blind image quality analyzer," *IEEE Signal Process. Lett.*, vol. 20, no. 3, pp. 209–212, Mar. 2013.